The Bcl10/paracaspase signalling complex is functionally conserved since the last common ancestor of planulozoa.

Jens Staal[1,2], Yasmine Driege[1,2], Paco Hulpiau[1,2], Rudi Beyaert[1,2]

[1] Inflammation Research Center, VIB, Ghent, Belgium

[2] Department of Biomedical Molecular Biology, Ghent University, Ghent, Belgium

Abstract

CARMA – CARDs, a single MALT1, cleavage and CLAP : an old story. The type 1 paracaspases are defined by their domain composition with an N-terminal Death-domain, immunoglobulin domains and a caspase-like (paracaspase) domain. Type 1 paracaspases originated in the Ediacaran geological period before the last common ancestor of bilaterans and cnidarians (planulozoa). Cnidarians have several paralog type 1 paracaspases, type 2 paracaspases, and a homolog of Bcl10 (CLAP). Notably in bilaterans, lineages like nematodes and insects lack Bcl10 whereas other lineages such as vertebrates, hemichordates, annelids and molluscs do contain Bcl10. A survey of invertebrate CARD-coiled-coil (CC) domain homologs of CARMA/CARD9 revealed such homologs only in species with Bcl10, indicating an ancient co-evolution of the entire CARD-CC/Bcl10/MALT1 (CBM) complex. There seems to be a correlation where invertebrates with CARD-CC and Bcl10 have type 1 paracaspases which are more similar to the paracaspases found in vertebrates. A proposed evolutionary scenario includes two ancestral type 1 paracaspase paralogs in the bilateran last common ancestor, where one paralog usually is dependent on CARD-CC/Bcl10 for its function. Functional analyses of invertebrate type 1 paracaspases and Bcl10 homologs support this scenario and indicate an ancient origin of the Bcl10/paracaspase signalling complex.

Introduction

The paracaspase MALT1 (PCASP1) was originally identified in humans as an oncogenic fusion with IAP2 in low-grade antibiotic-resistant MALT lymphomas[1]. Later, it was discovered that MALT1 is a critical component in T and B cell antigen receptor signalling as part of the CARMA1-Bcl10-MALT1 (CBM) complex[2 3 4]. More studies made it clear that MALT1 plays a role in several different CARD*-Bcl10-MALT1 complexes in many different types of signalling pathways, where currently known CARD* components are CARD9[5], CARD11 (CARMA1)[2], CARD14 (CARMA2)[6] and CARD10 (CARMA3)[7]. The use of the different CARD proteins in the CBM complexes is most likely mostly dependent on cell-type specific expression[8]. MALT1 was originally identified as a "paracaspase" due to sequence similarity with the true caspases and "metacaspases"[9]. The name caspase signifies both the structure (cysteine protease) and function (aspartic acid substrate specificity) of the protein family. The semantic association[10] of metacaspases and paracaspases to caspases is therefore unfortunate, since the similar names inspired false assumptions of common roles and properties of the different protein families[11]. It was not until much later that the proteolytic activity of MALT1 was established[12 13]. In contrast to true caspases (but similar to metacaspases and orthocaspases) the paracaspase MALT1 cleaves substrates specifically after an arginine residue[14 15 16]. Lately, some protein substrates have been identified which are cleaved after a lysine by the API2-MALT1 oncogenic fusion[17]. MALT1 cleaves itself[18] and its interacting adaptor protein Bcl10[13], the anti-inflammatory deubiquitinases A20[12] and CYLD[19], the NF-κB member RelB[20], the ubiquitin ligase HOIL-1[21 22 23] and the specific RNA degrading enzymes Regnase[24] and Roquin[25]. The anti-inflammatory role of many of the known protease substrates coupled with the critical role for MALT1 in inflammatory signalling has sparked an interest in

targeting MALT1 protease activity as a therapeutic strategy treatment of autoimmune diseases. The proteolytic activity of MALT1 was also found to be critical specifically for ABC-DLBCL B-cell lymphomas[26], which has sparked an interest in MALT1 protease activity also as a cancer therapy target. Although MALT1 has been clearly associated to NF-κB activity, its protease activity plays a more subtle role being specifically required for c-Rel activation[27 28 20 18]. There is some evidence that MALT1 also regulate or cross-talk with other pathways, such as JNK/AP-1[19], mTORC1[29] and possibly WNT[30]. MALT1 belongs to the type 1 paracaspase family, which consist of an N-terminal Death domain, immunoglobulin domains and a paracaspase domain[31]. The type 1 family of paracaspases originated sometime during the Ediacaran geological period, preceding the last common ancestor of bilaterans and cnidarians[32 31 33]. The cnidarians (e.g. jellyfish, anemone, hydra, coral, ...) and bilaterans (e.g. vertebrates, insects, nematodes, molluscs, ringed worms, …) form the planulozoan clade[34]. In our previous survey of paracaspases and MALT1-associated proteins, type 1 paracaspases and Bcl10 could not be found outside planulozoa[31]. Cnidarians typically contain several paralogs of both type 1 and the ancient type 2 paracaspases whereas bilaterans typically contain a single copy of a type 1 paracaspase. A notable exception is the jawed vertebrates, where the type 1 paracaspase got triplicated. Subsequently, two paralogs were lost in the mammalian lineage leaving PCASP1 (MALT1) as the single paracaspase in mammals[31]. Importantly, some organisms such as the nematode *Caenorhabditis elegans* contain a conserved type 1 paracaspase but lack NF-κB[35], which indicate that other roles or mechanisms might be responsible for the conservation of the general domain organization of the type 1 paracaspases[31]. On the other hand, despite the remarkable conservation of type 1 paracaspases, there are examples of bilaterans that have lost its paracaspase – most notable the group of flies that include *Drosophila melanogaster* (fruit fly)[31]. This indicates that alternative mechanisms can take over the unknown role which is usually filled by the type 1 paracaspases in most other planulozoan organisms. Apart from functional studies of MALT1 in human and mouse models, investigating the evolutionary history of the type 1 paracaspases and its interacting proteins in alternative model systems could provide important clues to yet-unknown roles and functions of MALT1[31]. Finding those alternative functions of MALT1 could be important for future MALT1 inhibitor-based therapies[36].

Materials & Methods

Sequences of type 1 paracaspases and Bcl10
Protein sequences of type 1 paracaspase, Bcl10 and CARMA/CARD9 homologs were retrieved from NCBI (https://www.ncbi.nlm.nih.gov), Ensembl (http://www.ensembl.org), JGI (http://genome.jgi.doe.gov/), OIST marine genomics (http://marinegenomics.oist.jp) [37 38 39] and ICMB (https://imcb.a-star.edu.sg) [40] using BLASTP [41]. All sequences used in the analyses can be found in supplemental material.

Sequence alignment and phylogenetic analysis
Sequence alignment was performed on the full sequence, using the different alignment algorithms MUSCLE (http://www.drive5.com/muscle/)[42], MAFFT (http://mafft.cbrc.jp/alignment/software/)[43] and T-coffee (http://www.tcoffee.org/)[44]. Phylogenetic analysis was performed with PHYLIP maximum-likelyhood (http://evolution.genetics.washington.edu/phylip.html)[45] and MrBayes (http://mrbayes.sourceforge.net/)[46] method. Both alignments and phylogenetic analyses were performed using UGENE (http://ugene.net/)[47] on Arch (http://www.archlinux.org) Linux[48]. For the figures, one of the most representative trees (alignment+phylogenetic analysis) was selected. For independent replication of the results, all sequences used in the phylogenetic analysis are available in the supplemental data. Metadata by colouring the branches was manually added along with manual adjustment of line thickness using inkscape (https://inkscape.org). The PCASP2 branch was also for aesthetic reasons manually rotated in the scalable vector graphics (svg) file without changing any branch

lengths in order to avoid overlapping branches.

Cloning of Bcl10 and paracaspase homologs
Plasmids of the cloned genes were deposited in the BCCM/LMBP plasmid collection along with detailed descriptions of cloning strategy and plasmid sequence (http://bccm.belspo.be/about-us/bccm-lmbp). The starlet sea anemone (*Nematostella vectensis*) type 1 paracaspase paralog "A" (LMBP: 9589) and zebrafish PCASP3 (LMBP: 9573) were cloned previously[31]. The *Nematostella* type 1 paracaspase paralogs "A" (LMBP: 9636) and "B" (LMBP: 9825) and pacific oyster (*Crassostrea gigas*, LMBP: 9826) were cloned behind the human ETV6 HLH domain for dimerization-induced activation as described previously[49 18 31]. Human (LMBP: 9637), zebrafish (LMBP: 9665), pacific oyster (LMBP: 9666) and *Nematostella* (LMBP: 9822) Bcl10 were cloned in the pCAGGS vector with an N-terminal E-tag.

Cell culture, transfection and expression analysis
MALT1 KO HEK293T cells (clone #39)[31] were grown under standard conditions (DMEM, 10% FCS, 5% CO_2, 37 °C) and transfected with the calcium phosphate method [50].
For evaluation of the conservation of cleavage activity, the HLH-fused paracaspase constructs were co-transfected with wild-type CYLD (LMBP: 6613) or the uncleavable CYLD-R324A (LMBP: 6645) mutant. Cells transfected for cleavage activity evaluations were lysed directly in Laemmli buffer (0.1% 2-Mercaptoethanol, 5ppm Bromophenol blue, 10% Glycerol, 2% SDS, 63 mM Tris-HCl (pH 6.8)).
For evaluation of conservation of NF-κB induction, the HLH paracaspase fusions were co-transfected with a NF-κB luciferase reporter (LMBP: 3249) and actin promoter-driven β-galactosidase (LMBP: 4341) as transfection control. The cells used for luciferase analysis were washed with 1XPBS and lysed in luciferase lysis buffer (25mM Tris pH7.8, 2mM DTT, 2mM CDTA, 10% glycerol, 1% Triton X-100). For the colorimetric determination (at 595nm) of β-galactosidase activity, chlorophenol red-β-D-galactopyranoside (CPRG) (Roche diagnostics) was used as a substrate. The luciferase activity was measured by using beetle luciferin (Promega) as a substrate and the luminescence was measured with the GloMax® 96 Microplate Luminometer (Promega). Luciferase data processing and calculation of 95% confidence intervals (Student's t-distribution[51]) was done in Libreoffice (www.libreoffice.org) Calc.
For evaluation of the functional conservation of the Bcl10 homologs, the Bcl10 clones were co-transfected with the NF-κB luciferase reporter and β-galactosidase in the MALT1 KO HEK293T cells with or without reconstitution with human MALT1 (LMBP: 5536). Detection of cleaved CYLD was done with the E10 antibody (Santa Cruz Biotechnology) recognizing the C-terminal 70kDa cleavage band or anti-E-tag (ab66152, Abcam) recognizing the 40kDa N-terminal cleavage band. Expression of the fused paracaspases was determined with anti-Flag (F-3165, Sigma). Human MALT1 was detected by the EP603Y monoclonal rat antibody (Abcam) and the E-tagged Bcl10 clones with anti-E-tag. All western blots were developed on an Odyssey scanner (LI-COR).

Results & Discussion
Correlation vertebrate-like type 1 paracaspases and presence of Bcl10.
While searching for invertebrate homologs of type 1 paracaspases and Bcl10, it became apparent that type 1 paracaspases from species containing Bcl10 generally had higher BLASTP rankings compared to species from phyla lacking Bcl10. Bcl10 sequences in vertebrates appear to evolve in a manner similar to how the species have diverged throughout evolution (frog being an exception[31]), while the invertebrate Bcl10 sequences are poorly resolved (Figure 1A). To get a better understanding of early Bcl10 evolution, more sequences from invertebrate genomes are needed. Different alignment strategies (MAFFT[43], MUSCLE[42], T-Coffee[44]) and phylogenetic analyses (PHYLIP[45], MrBayes[46]) of several type 1 paracaspases verify that type 1 paracaspases from species that contain

Bcl10 (molluscs, annelids, hemichordates) often cluster closer to the vertebrate paracaspases, either directly or indirectly by clustering with the vertebrate PCASP3 orthologs from tunicate and lancelet[31] (Figure 1B), indicating a conserved common Bcl10-dependent ancestor. We can currently not resolve whether there were two paracaspase paralogs, one Bcl10-dependent and the other Bcl10-independent already from the planulozoan last common ancestor or if Bcl10-independent paralogs have evolved several times. In the second model, a Bcl10-independent paralog would have evolved early on in the bilateran evolution. Since the cnidarian paracaspases tend to cluster together in most models, we expect that the last common bilateran ancestor had a single Bcl10-dependent type 1 paracaspase.

Functional conservation of invertebrate type 1 paracaspases and Bcl10
Based on BLASTP, the mollusc paracaspases were identified as the non-deuterostome homologs most closely resembling vertebrate type 1 paracaspases[31]. Based on top-ranking BLASTP hits, the pacific sea oyster (*Crassostrea gigas*)[52] was selected as a model and cDNA source for the molluscs. Conversely, the most distantly related species where type 1 paracaspases and Bcl10 could be found are cnidaria[31]. The cnidarian model organism starlet sea anemone (*Nematostella vectensis*)[53] was used as a cDNA source for as divergent homologous proteins as possible. In order to investigate the functional conservation of invertebrate type 1 paracaspases, we evaluated artificially activated type 1 paracaspases fused to the ETV6 HLH domain[18]. As positive control, the currently most distantly related vertebrate paracaspase with conserved activity (zebrafish PCASP3)[31] was used. In an NF-κB luciferase assay, only the activated zebrafish PCASP3 could induce the reporter to relevant levels, indicating that the pacific oyster (CgPCASP) and the two starlet sea anemone type 1 paracaspase paralogs (NvPCASP-t1A, NvPCASP-t1B) could not recruit critical downstream signalling components (Figure 2A). Although a statistically significant NF-κB induction could be seen from CgPCASP, the levels were more than 150-fold less than what is observed from vertebrate paracaspases and probably not relevant (Figure 2A). In contrast, evaluation of protease activity revealed that the pacific oyster paracaspase specifically cleaves human CYLD at R324, just like vertebrate paracaspases (Figure 2B). This differs from our previous studies of invertebrate paracaspases such as the type 1 paracaspase from *C. elegans* and the more distantly related type 2 paracaspases, which failed to show any activity[31]. On the other hand, the "A" type 1 paracaspase paralog from starlet sea anemone could not cleave CYLD at all and the "B" paralog appeared to cleave CYLD, but at a different residue, indicating that paracaspase substrate specificity is not conserved in the cnidarians. To further investigate the functional conservation of the Bcl10/paracaspase co-evolution, we transfected human, zebrafish, pacific oyster and starlet sea anemone Bcl10 in MALT1 KO HEK293T cells with or without reconstitution with human MALT1. Strikingly, the starlet sea anemone Bcl10 could induce human MALT1-mediated NF-κB induction. In contrast to human and zebrafish Bcl10, NvBcl10 does not appear to be cleaved by human MALT1 (Figure 2C). The pacific oyster Bcl10 failed to induce any NF-κB reporter activity, which might be due to its small size. It will be interesting to see if future annotations of the mollusc genomes will establish a longer Bcl10 transcript encoding for a functional Bcl10 homolog[54].

Conservation and co-evolution of the CBM complex
Previous studies has shown that the MALT1-like activities are conserved at least as far back as the last common ancestor of the three vertebrate type 1 paracaspase paralogs[31]. Similarly, also Bcl10 has been shown to be functionally conserved as far back as zebrafish[55]. We also know that the upstream interaction to CARMA proteins is conserved at least as far back as zebrafish[55]. We have now shown that Bcl10 and MALT1-like activities from type 1 paracaspases are considerably older, most likely preceding the Cambrian explosion[34]. The observation that invertebrate type 1 paracaspases from organisms that also contain Bcl10 are more similar to the vertebrate paracaspases

provides a new interesting perspective on the functional evolution of MALT1. CARMA proteins are unique to vertebrates, but the conserved CARD-coiled-coil (CC) domain can be found in some invertebrates. Intriguingly, also these CARMA/CARD9-related CARD-CC domain proteins show a phylogenetic distribution which is similar to Bcl10 (Figure 3), indicating that the entire CARD-CC/Bcl10/MALT1 (CBM) complex is co-evolving and that species with Bcl10-independent type 1 paracaspases rely on a completely independent activation mechanism. The placement of CARD14 (CARMA2) at the base of the CARMA/CARD9 proteins found in vertebrates based on the CARD domain phylogeny (Figure 3) is consistent with phylogenies made with the MAGUK domain[56], indicating that CARD14 might be the ancestral CARMA in vertebrates. A likely evolutionary scenario for the CARMA proteins is that a CARD9-like CARD-CC got fused with a ZO-1/Dlg5-like MAGUK protein upstream of the PDZ domain early in the vertebrate evolution. Interestingly, the presence of 3 CARMA paralogs and 3 type 1 paracaspase paralogs in the vertebrate lineage both seem to have arisen in the last common ancestor of jawed vertebrates. Lampreys only seem to have a single ancestral CARD-CC (Figure 3) and a single type 1 paracaspase which seems to be the parent of the PCASP3 and PCASP2/1 branches in jawed vertebrates (Figure 1). Surprisingly, the supposedly ancestral CARD-CC in lampreys is clustering closer to CARD11 than CARD14.

Future challenges
We still don't know how far back that MALT1-like activities such as TRAF6 interaction and NF-κB induction, protease activity and specificity are conserved. With the observation that mollusc paracaspases have conserved protease activity and specificity, but fail to induce NF-κB in a human cellular background, we are starting to unravel the sequence of evolutionary events leading to the current MALT1 activities in humans. The observation that cnidarian Bcl10 can activate human MALT1 indicates a highly conserved interaction surface between the two proteins. This type of conservation could be used to further model the interaction surfaces using evolutionary data[57]. A major future challenge will be to collect and functionally evaluate more invertebrate type 1 paracaspase, Bcl10 and CARD-CC homologs to verify the proposed correlation of a CARD-CC/Bcl10-dependent ancestral type 1 paracaspase paralog with MALT1-like activity and to model the evolution of the MALT1-Bcl10 interaction. There are several aspects that are yet not clear, for example can no Bcl10 homolog currently be found in lancelets, which clearly have a PCASP3 ortholog [31]. The limited number of invertebrate true Bcl10 homologs that can be identified in public sequence data is currently a clear limitation for further analysis. CRADD homologs often are picked up as false positives since they contain a CARD domain that is very similar to Bcl10[58] [59]. The current model proposes an ancient parallel evolution of a Bcl10-dependent and a Bcl10-independent paracaspase (Figure 4). An alternative scenario is that Bcl10-independence has evolved several times independently. In order to further clarify this, more invertebrate sequences from informative phyla are needed[60]. Several proteins associated to MALT1 in humans are conserved as far back as cnidarians, such as CARMA/CARD9, Bcl10, TRAF6, TRAF2 and CYLD[31]. Investigating early-diverging biological systems such as the cnidarian model organism *Nematostella vectensis* for protein interactions and signal transduction mechanisms could further pin-point the original and most conserved functions. Another highly interesting model organism to study would be the nematode *C. elegans* to specifically investigate the CARD-CC/Bcl10- and NF-κB independent functions of type 1 paracaspases in bilaterans.

Acknowledgements

Supplemental material

Supplemental text 1 : FASTA sequences of type 1 paracaspases used in phylogeny

Supplemental text 2 : FASTA sequences of Bcl10 homologs used in phylogeny

Supplemental text 3 : FASTA sequences of CARMA/CARD9 homologs used in phylogeny

References

1. Dierlamm, J. *et al.* The Apoptosis Inhibitor Gene API2 and a Novel 18q Gene,MLT, Are Recurrently Rearranged in the t(11;18)(q21;q21) Associated With Mucosa-Associated Lymphoid Tissue Lymphomas. *Blood* **93,** 3601–3609 (1999).

2. Che, T. *et al.* MALT1/paracaspase is a signaling component downstream of CARMA1 and mediates T cell receptor-induced NF-kappaB activation. *J. Biol. Chem.* **279,** 15870–15876 (2004).

3. Ruefli-Brasse, A. A., French, D. M. & Dixit, V. M. Regulation of NF-kappaB-dependent lymphocyte activation and development by paracaspase. *Science* **302,** 1581–4 (2003).

4. Ruland, J., Duncan, G. S., Wakeham, A. & Mak, T. W. Differential requirement for Malt1 in T and B cell antigen receptor signaling. *Immunity* **19,** 749–58 (2003).

5. Gross, O. *et al.* Card9 controls a non-TLR signalling pathway for innate anti-fungal immunity. *Nature* **442,** 651–6 (2006).

6. Schmitt, A. *et al.* MALT1 Protease Activity Controls the Expression of Inflammatory Genes in Keratinocytes upon Zymosan Stimulation. *J. Invest. Dermatol.* **136,** 788–797 (2016).

7. McAllister-Lucas, L. M. *et al.* CARMA3/Bcl10/MALT1-dependent NF-kappaB activation mediates angiotensin II-responsive inflammatory signaling in nonimmune cells. *Proc Natl Acad Sci U A* **104,** 139–44 (2007).

8. Scudiero, I., Vito, P. & Stilo, R. The Three CARMA Sisters: So Different, So Similar. A Portrait of the Three CARMA Proteins and their Involvement in Human Disorders. *J. Cell. Physiol.* (2013). doi:10.1002/jcp.24543

9. Uren, A. G. *et al.* Identification of paracaspases and metacaspases: two ancient families of caspase-like proteins, one of which plays a key role in MALT lymphoma. *Mol Cell* **6,** 961–7 (2000).

10. Wedgwood, D. Shared assumptions: Semantic minimalism and Relevance Theory. *J. Linguist.* **43,** 647–681 (2007).

11. Salvesen, G. S., Hempel, A. & Coll, N. S. Protease signaling in animal and plant-regulated cell death. *FEBS J.* (2015). doi:10.1111/febs.13616

12. Coornaert, B. *et al.* T cell antigen receptor stimulation induces MALT1 paracaspase-mediated cleavage of the NF-kappaB inhibitor A20. *Nat Immunol* **9,** 263–71 (2008).

13. Rebeaud, F. *et al.* The proteolytic activity of the paracaspase MALT1 is key in T cell activation.

Nat Immunol **9,** 272–81 (2008).

14. Hachmann, J. *et al.* Mechanism and specificity of the human paracaspase MALT1. *Biochem. J.* **443,** 287–295 (2012).

15. Yu, J. W., Jeffrey, P. D., Ha, J. Y., Yang, X. & Shi, Y. Crystal Structure of the Mucosa-Associated Lymphoid Tissue Lymphoma Translocation 1 (MALT1) Paracaspase Region. *Proc. Natl. Acad. Sci.* **108,** 21004–21009 (2011).

16. Wiesmann, C. *et al.* Structural Determinants of MALT1 Protease Activity. *J. Mol. Biol.* **419,** 4–21 (2012).

17. Nie, Z. *et al.* Conversion of the LIMA1 tumour suppressor into an oncogenic LMO-like protein by API2-MALT1 in MALT lymphoma. *Nat. Commun.* **6,** 5908 (2015).

18. Baens, M. *et al.* MALT1 auto-proteolysis is essential for NF-κB-dependent gene transcription in activated lymphocytes. *PloS One* **9,** e103774 (2014).

19. Staal, J. *et al.* T-cell receptor-induced JNK activation requires proteolytic inactivation of CYLD by MALT1. *EMBO J.* **30,** 1742–1752 (2011).

20. Hailfinger, S. *et al.* Malt1-Dependent RelB Cleavage Promotes Canonical NF-κB Activation in Lymphocytes and Lymphoma Cell Lines. *Proc. Natl. Acad. Sci.* **108,** 14596–14601 (2011).

21. Elton, L. *et al.* MALT1 cleaves the E3 ubiquitin ligase HOIL-1 in activated T cells, generating a dominant negative inhibitor of LUBAC-induced NF-κB signaling. *FEBS J.* (2015). doi:10.1111/febs.13597

22. Klein, T. *et al.* The paracaspase MALT1 cleaves HOIL1 reducing linear ubiquitination by LUBAC to dampen lymphocyte NF-κB signalling. *Nat. Commun.* **6,** 8777 (2015).

23. Douanne, T., Gavard, J. & Bidère, N. The paracaspase MALT1 cleaves the LUBAC subunit HOIL1 during antigen receptor signaling. *J. Cell Sci.* (2016). doi:10.1242/jcs.185025

24. Uehata, T. *et al.* Malt1-Induced Cleavage of Regnase-1 in CD4+ Helper T Cells Regulates Immune Activation. *Cell* **153,** 1036–1049 (2013).

25. Jeltsch, K. M. *et al.* Cleavage of roquin and regnase-1 by the paracaspase MALT1 releases their cooperatively repressed targets to promote T(H)17 differentiation. *Nat. Immunol.* **15,** 1079–1089 (2014).

26. Fontan, L. *et al.* MALT1 small molecule inhibitors specifically suppress ABC-DLBCL in vitro and in vivo. *Cancer Cell* **22,** 812–824 (2012).

27. Ferch, U. *et al.* MALT1 directs B cell receptor-induced canonical nuclear factor-kappaB
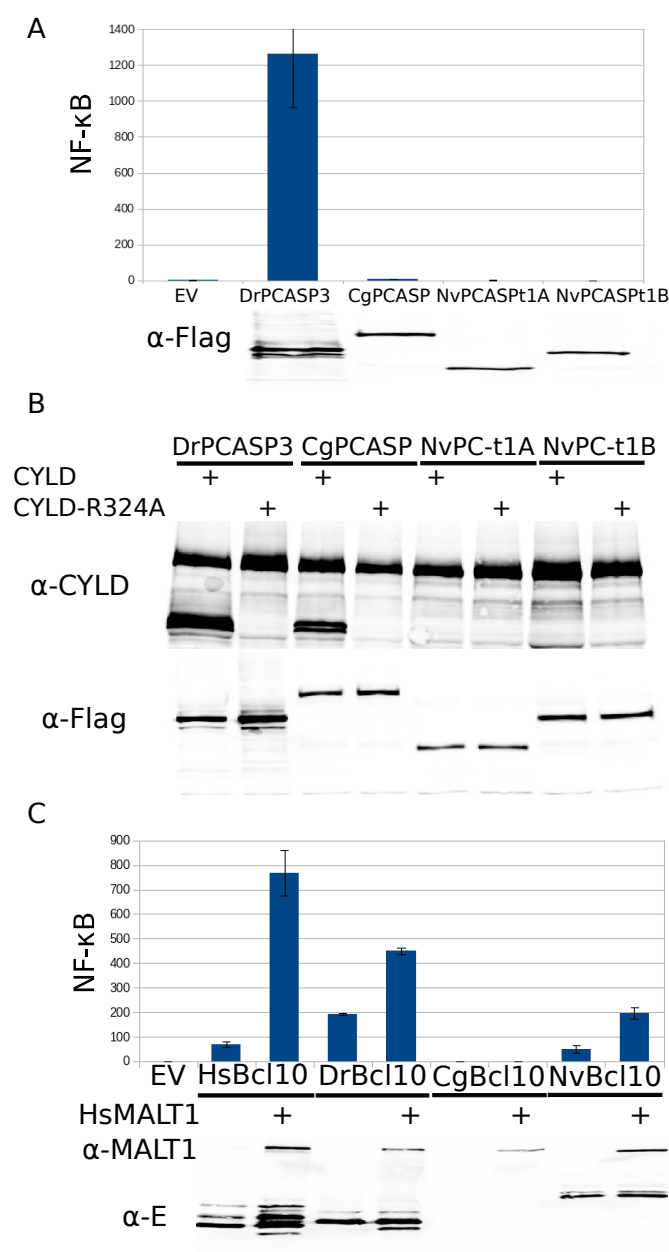
signaling selectively to the c-Rel subunit. *Nat. Immunol.* **8,** 984–991 (2007).

28. Gringhuis, S. I. *et al.* Selective C-Rel activation via Malt1 controls anti-fungal T(H)-17 immunity by dectin-1 and dectin-2. *PLoS Pathog.* **7,** e1001259 (2011).

29. Hamilton, K. S. *et al.* T cell receptor-dependent activation of mTOR signaling in T cells is mediated by Carma1 and MALT1, but not Bcl10. *Sci. Signal.* **7,** ra55 (2014).

30. Bognar, M. K. *et al.* Oncogenic CARMA1 couples NF-κB and β-catenin signaling in diffuse large B-cell lymphomas. *Oncogene* (2016). doi:10.1038/onc.2015.493

31. Hulpiau, P., Driege, Y., Staal, J. & Beyaert, R. MALT1 is not alone after all: identification of novel paracaspases. *Cell. Mol. Life Sci. CMLS* (2015). doi:10.1007/s00018-015-2041-9

32. Knoll, A., Walter, M., Narbonne, G. & Christie-Blick, N. The Ediacaran Period: a new addition to the geologic time scale. *Lethaia* **39,** 13–30 (2006).

33. Peterson, K. J. *et al.* Estimating metazoan divergence times with a molecular clock. *Proc. Natl. Acad. Sci. U. S. A.* **101,** 6536–6541 (2004).

34. Dunn, C. W., Giribet, G., Edgecombe, G. D. & Hejnol, A. Animal Phylogeny and Its Evolutionary Implications. *Annu. Rev. Ecol. Evol. Syst.* **45,** 371–395 (2014).

35. Sullivan, J. C. *et al.* Two Alleles of NF-?B in the Sea Anemone Nematostella vectensis Are Widely Dispersed in Nature and Encode Proteins with Distinct Activities. *PLoS ONE* **4,** (2009).

36. Demeyer, A., Staal, J. & Beyaert, R. Targeting MALT1 Proteolytic Activity in Immunity, Inflammation and Disease: Good or Bad? *Trends Mol. Med.* (2016). doi:10.1016/j.molmed.2015.12.004

37. Shinzato, C. *et al.* Using the Acropora digitifera genome to understand coral responses to environmental change. *Nature* **476,** 320–323 (2011).

38. Luo, Y.-J. *et al.* The Lingula genome provides insights into brachiopod evolution and the origin of phosphate biomineralization. *Nat. Commun.* **6,** 8301 (2015).

39. Simakov, O. *et al.* Hemichordate genomes and deuterostome origins. *Nature* **527,** 459–465 (2015).

40. Venkatesh, B. *et al.* Elephant shark genome provides unique insights into gnathostome evolution. *Nature* **505,** 174–179 (2014).

41. Johnson, M. *et al.* NCBI BLAST: a better web interface. *Nucleic Acids Res.* **36,** W5-9 (2008).

42. Edgar, R. C. MUSCLE: multiple sequence alignment with high accuracy and high throughput. *Nucleic Acids Res.* **32,** 1792–1797 (2004).

43. Katoh, K., Misawa, K., Kuma, K. & Miyata, T. MAFFT: a novel method for rapid multiple sequence alignment based on fast Fourier transform. *Nucleic Acids Res.* **30,** 3059–3066 (2002).

44. Notredame, C., Higgins, D. G. & Heringa, J. T-Coffee: A novel method for fast and accurate multiple sequence alignment. *J. Mol. Biol.* **302,** 205–217 (2000).

45. Felsenstein, J. Evolutionary trees from DNA sequences: a maximum likelihood approach. *J. Mol. Evol.* **17,** 368–376 (1981).

46. Ronquist, F. & Huelsenbeck, J. P. MrBayes 3: Bayesian phylogenetic inference under mixed models. *Bioinforma. Oxf. Engl.* **19,** 1572–1574 (2003).

47. Okonechnikov, K., Golosova, O., Fursov, M. & UGENE team. Unipro UGENE: a unified bioinformatics toolkit. *Bioinforma. Oxf. Engl.* **28,** 1166–1167 (2012).

48. Torvalds, L. The Linux Edge. *Commun ACM* **42,** 38–39 (1999).

49. Malinverni, C. *et al.* Cleavage by MALT1 induces cytosolic release of A20. *Biochem. Biophys. Res. Commun.* **400,** 543–547 (2010).

50. Calcium phosphate–mediated transfection of eukaryotic cells. *Nat. Methods* **2,** 319–320 (2005).

51. Student. The probable error of a mean. *Biometrika* **6,** 1–25 (1908).

52. Zhang, G. *et al.* The oyster genome reveals stress adaptation and complexity of shell formation. *Nature* **490,** 49–54 (2012).

53. Darling, J. A. *et al.* Rising starlet: the starlet sea anemone, Nematostella vectensis. *BioEssays News Rev. Mol. Cell. Dev. Biol.* **27,** 211–221 (2005).

54. Riviere, G. *et al.* GigaTON: an extensive publicly searchable database providing a new reference transcriptome in the pacific oyster Crassostrea gigas. *BMC Bioinformatics* **16,** 401 (2015).

55. Mazzone, P. *et al.* Functional characterization of zebrafish (Danio rerio) Bcl10. *PloS One* **10,** e0122365 (2015).

56. de Mendoza, A., Suga, H. & Ruiz-Trillo, I. Evolution of the MAGUK protein gene family in premetazoan lineages. *BMC Evol. Biol.* **10,** 93 (2010).

57. Hopf, T. A. *et al.* Sequence co-evolution gives 3D contacts and structures of protein complexes. *eLife* **3,** (2014).

58. Lin, Q. *et al.* Cutting edge: the 'death' adaptor CRADD/RAIDD targets BCL10 and suppresses agonist-induced cytokine expression in T lymphocytes. *J. Immunol. Baltim. Md 1950* **188,** 2493–2497 (2012).

59. Qiao, H., Liu, Y., Veach, R. A., Wylezinski, L. & Hawiger, J. The adaptor CRADD/RAIDD controls activation of endothelial cells by proinflammatory stimuli. *J. Biol. Chem.* **289,** 21973–21983 (2014).

60. Scientists, G. C. of. The Global Invertebrate Genomics Alliance (GIGA): Developing Community Resources to Study Diverse Invertebrate Genomes. *J. Hered.* **105,** 1–18 (2014).

Figure 1
Phylogeny of Bcl10 and type 1 paracaspases

Species key: <u>Vertebrates</u>: Hs=Human, Mm=mouse, Gg=Chicken, Pb=Python, Ac=anole lizard Xt=African clawed frog, Dr=Zebrafish, Tr=Fugu, Cm=Elephant shark, Pm=Sea lamprey. <u>Tunicates:</u> Ci=Vase tunicate <u>Lancelets:</u> Bf=Florida lancelet. <u>Hemichordates:</u> Sk=Acorn worm Pf=Hawaiian acorn worm <u>Molluscs:</u> Cg=Pacifc oyster, Lg=Limpet, Ob=Califonia two-spot octopus <u>Brachiopods</u>: La=*L. anatina* <u>Annelids:</u> Ct=polychaete worm <u>Arthropods:</u> Dp=Water flea, Am=Honey bee, Sm=African social velvet spider, Is=Fire ant, Ls=salmon louse <u>Cnidaria:</u> Nv=Starlet sea anemone, Hm=Hydra, Ad=Stag horn coral
A) A representative phylogenetic tree of Bcl10 (MAFFT+MrBayes): Vertebrate sequences highlighted with red branches.
B) A representative phylogenetic tree (MAFFT+MrBayes) of the type 1 paracaspases: Vertebrate paracaspases highlighted with red branches, paracaspases from invertebrate species with Bcl10 with purple branches and species from phyla completely lacking Bcl10 (arthropods, nematodes) with blue.

Figure 2
Functional conservation of invertebrate paracaspase and Bcl10

A) NF-κB induction by activated HLH-paracaspase fusions expressed in MALT1 KO HEK293T cells. Luciferase values are normalized against β-galactosidase and expressed as fold induction compared to samples not expressing a HLH-paracaspase fusion (EV). Error bars represent 95% confidence intervals. **B**) CYLD cleavage by activated HLH-paracaspase fusions. Human CYLD is specifically cleaved by vertebrate paracaspases after residue R324, resulting in a 70kDa C-terminal fragment and a 40kDa N-terminal fragment. Cleavage of WT CYLD but failure to cleave the R324A mutant indicate a conserved substrate specificity. **C**) Human MALT1-dependent NF-κB induction by different Bcl10 homologs. The different Bcl10 homologs were expressed in MALT1 KO HEK293T cells. Bcl10 induces NF-κB via MALT1, which is illustrated by the increase of luciferase activity when the cells are reconstituted with human MALT1. Luciferase values are normalized against β-galactosidase and expressed as fold induction compared to samples not expressing Bcl10 (EV). Error bars represent 95% confidence intervals (Student's t-distribution). All experiments were repeated at least twice.

Figure 3

Evolution of CARD9/CARMA-homologs

Species key: <u>Vertebrates</u>: Hs=Human, Gg=Chicken, Xt=African clawed frog, Dr=Zebrafish, Cm=Elephant shark, Pm=Sea lamprey, Jl=Japanese lamprey <u>Tunicates:</u> Ci=vase tunicate <u>Hemichordates:</u> Sk=Acorn worm <u>Molluscs:</u> Cg=Pacifc oyster <u>Annelids:</u> Ct=polychaete worm, Hr=leech <u>Cnidaria:</u> Nv=Starlet sea anemone, Hm=Hydra, Ep=Sea anemone

A representrative tree (MUSCLE+MrBayes) showing the relationships between CARD9, the CARMA paralogs and its invertebrate CARD-CC homologs. The invertebrate homologs have been named based on their top vertebrate BLASTP hit. Red branches highlight vertebrate sequences, blue branches cnidaria and green branches annelids.
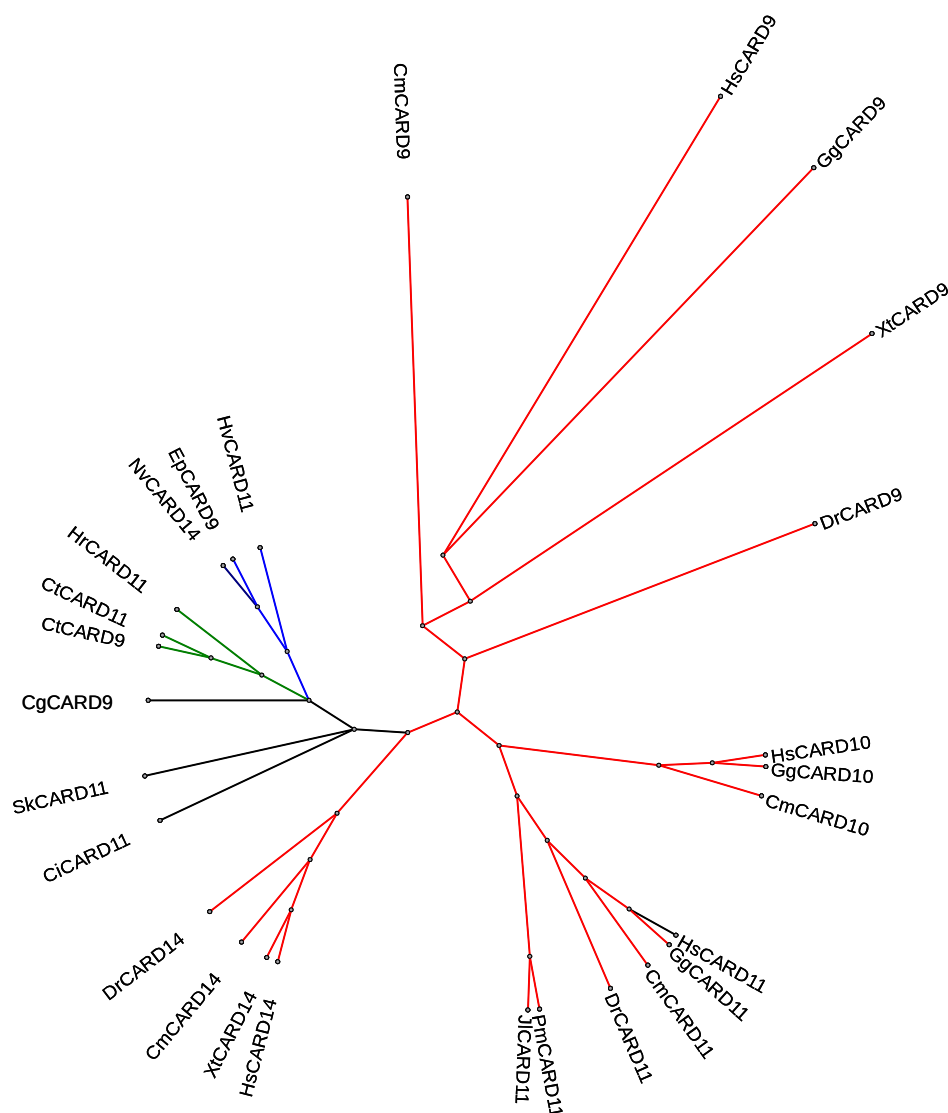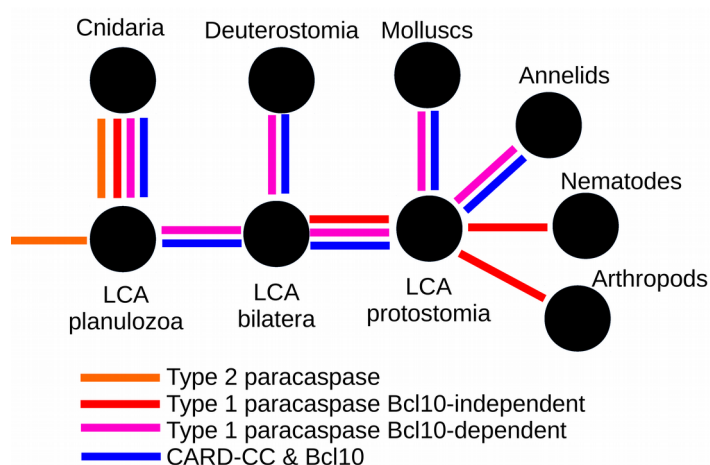
Figure 4
Proposed model

A model that proposes 2 ancient type 1 paracaspases, one Bcl10-dependent and one Bcl10-independent. The CARD-CC/Bcl10-dependent type 1 paracaspase shows MALT1-like activities. Deuterostomia (including tunicates, lancelets, vertebrates and hemichordates like the acorn worm), annelids and molluscs inherited the Bcl10-dependent type 1 paracaspase whereas most other bilateran invertebrates kept the Bcl10-independent type 1 paracaspase. The model is based on currently available reliable sequence information and might change with additional data.